Available online at www.sciencedirect.com

ScienceDirect

Procedia Chemistry 1 (2009) 1063–1066

Procedia Chemistry

www.elsevier.com/locate/procedia

Proceedings of the Eurosensors XXIII conference

Mass Sensing using an Amorphous Silicon MEMS resonator

S. B. Patil[a], V. Chu[a], J. P. Conde[a,b]*

[a]*INESC Microsistemas e Nanotecnologias (INESC MN) and IN-Institute of Nanoscience and Nanotechnology, Rua Alves Redol, 9, Lisbon 1000-029, Portugal*

[b]*Department of Chemical and Biological Engineering, Instituto Superior Técnico, Av. Rovisco Pais 1, Lisbon 1049-001, Portugal*

Abstract

Bilayer micro-bridge resonators of amorphous silicon and titanium were fabricated on a glass substrate at 100°C by surface micromachining using an aluminum sacrificial layer. Au square patterns with sub-micrometer dimensions were patterned on top of the microresonators. These Au squares allowed specific immobilization of thiolated single strand DNA probe oligonucleotides. The frequency response of the electrostatically-actuated resonators was measured optically. The mass loading effect of the Au squares and of the immobilized ssDNA probes were determined by the shift in the resonance frequency of the micro-bridge resonators.

Keywords: MEMS resonators, amorphous silicon and mass sensing.

1. Introduction

Microelectromechanical systems (MEMS) with various designs and approaches have been used as microbalances to detect the mass of the species attached to the MEMS structure with mass sensitivities ranging from picograms to zeptograms [1-4]. These MEMS structures were in general fabricated either by surface micromachining on crystalline silicon substrates with polysilicon used as a structural layer and thermally grown SiO_2 as a sacrificial layer at processing temperatures above 700°C, or by bulk micromachining of a silicon wafer. High temperature processing limits integration of the MEMS with control electronics on the same chip to reduce the cost and the size of the end product. As an alternative technology, MEMS based on hydrogenated amorphous silicon (a-Si:H) thin film-based structural layers deposited by PECVD at low temperatures (between 100 and 250°C) has been proposed [5,6]. The low processing temperatures allow the fabrication of MEMS on alternative substrates such as glass or plastic. The low temperature processing also makes this technology CMOS compatible. In this paper, the results for the mass sensing of 1) Au squares with submicron dimensions patterned on top of the a-Si:H/TiW bilayer microresonators; and 2) the effect of the immobilization of thiolated ssDNA probes on the Au surfaces, are presented.

* Corresponding author. Tel: +351-21-8419632, Fax: +351-21-8499242.
E-mail address: joao.conde@ist.utl.pt

doi:10.1016/j.proche.2009.07.265

2. Experimental

Fig.1(a) shows the fabrication process sequence for the bilayer (a-Si:H/TiW) MEMS resonators (with length L = 15 μm and width w = 5 μm) on a glass substrate using Al as a sacrificial layer. The TiW (100 nm) layer is deposited by DC magnetron sputtering and patterned to form the gate electrode using photolithography and wet etching with an Al hard mask (fig. 1(a)-1). The Al sacrificial layer (750 nm) is deposited by DC magnetron sputtering and patterned using wet etching (fig. 1(a)-2). A thin TiW (10 nm) was deposited on top of the Al sacrificial layer as a diffusion barrier between the sacrificial (Al) and the structural layer (a-Si:H) to avoid silicide formation and to facilitate the later removal of the sacrificial material. The structural material of the microbridge consists of a bilayer of n-type doped amorphous silicon (200 nm) deposited by RF-PECVD and a TiW (50 nm) layer as a top contact (fig. 1(a)-3). Before patterning the bridge, a 100 nm thick Au layer was deposited on top and patterned by e-beam lithography as squares with edge lengths varying between 100 nm and 2 μm. After the patterning of the microbridges, the Al sacrificial layer was selectively removed by Al etchant.

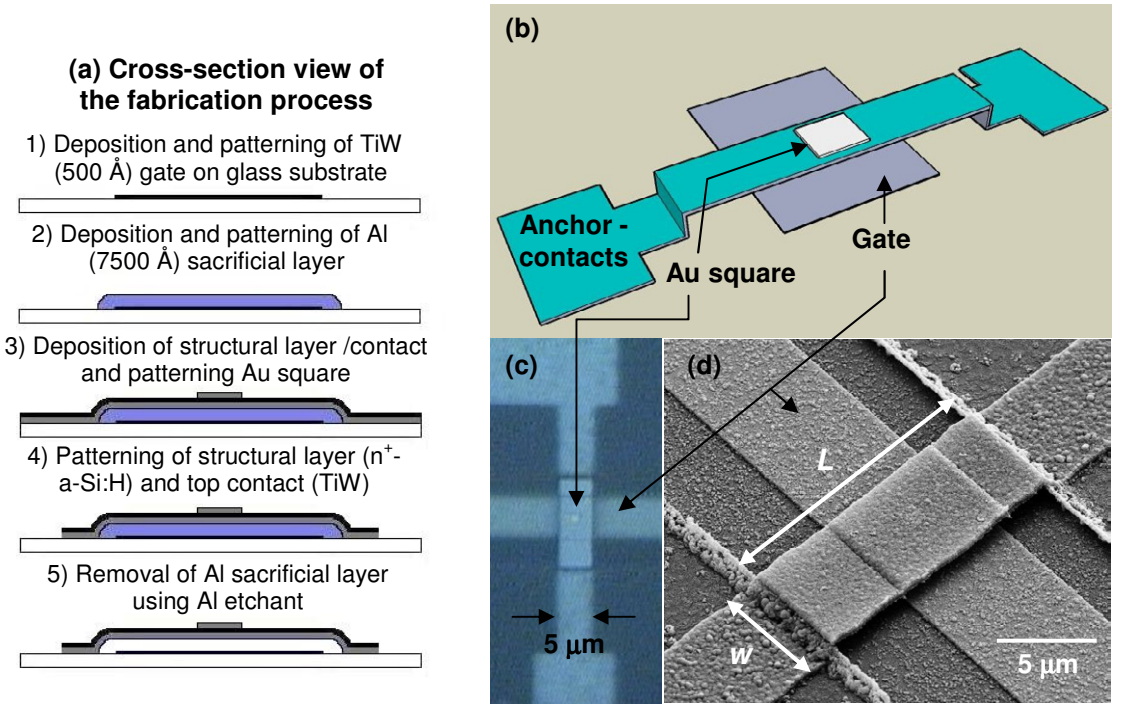

Fig. 1 (a) Cross-section view of the fabrication process sequence of the amorphous silicon MEMS resonator; b) schematic of the micro-resonator bridge (length L = 15 μm and width w = 5 μm) with an Au square patterned on top; c) optical micrograph of a microbridge with a 1.4 μm × 1.4 μm Au square on top; and d) SEM micrograph of a microbridge (in this case, a reference structure, without a patterned Au square on top).

Figs. 1(b) and 1(c) show a schematic and an optical micrograph, respectively, of the micro-bridge with an Au square (1.4 μm × 1.4 μm) on top. Fig. 1(d) shows a SEM micrograph of a micro-bridge. The micro-bridge resonators were electrostatically actuated by applying a voltage, V_G, between the gate electrode and the bridge. V_G has DC and AC components, and can be described as $V_G = V_{DC} + V_{AC}\sin(2\pi ft)$, where $V_{DC} >> V_{AC}$, and f is the excitation frequency. The resulting deflection in vacuum is monitored by means of an optical setup described elsewhere [7] at a pressure of ~10^{-6} Torr,

2. Results and discussion

The resonance frequency, f_r, for the micro-bridge resonator can be given approximately by eq. (1):

$$f_r = \frac{1}{2\pi}\sqrt{\pi^4\left(a_n+\frac{1}{2}\right)^4\frac{(EI)_{eff}}{\mu_{eff}L^4}+\pi^2\left(a_n+\frac{1}{2}\right)^2\sigma_0\frac{wt_{eff}}{\mu_{eff}L^2}} \quad (1)$$

where $a_n = a_1 = 1.00562$ for the first flexural mode of a clamped-clamped bridge [7], μ_{eff} is the mass per unit length of the suspended microbridge structure, t_{eff} is the total thickness of the microbridge, w is width, and L is the length of the structure. The first term in eq. (1) represents the contribution of the rigidity, $(EI)_{eff}$, of the structure and the second term the contribution from the residual axial stress, σ_0, in a micro-bridge to f_r. E is the Young´s modulus of the composite structure (a function of the Young´s modulus for a-Si:H, E_1= 150 GPa, and for TiW, E_2=450 GPa) and I is moment of inertia of the structure. In the absence of axial stress, $\sigma_0 = 0$, the change in f_r, Δf_r, due to the added mass Δm on top of the micro-resonator is given by (if one assumes that the added mass does not contribute to the rigidity of the micro-bridge structure) [1]:

$$\Delta f_r = -\frac{1}{2}\frac{\Delta m}{m} f_i \quad (2)$$

where f_i is the initial resonance frequency of the micro-bridge resonator before addition of the extra mass.

For the micro-bridges studied, the spring constant k ($k = 3(EI)_{eff}/L^3$, in the absence of residual stresses) and the mass (without Au squares on top) are 1.82 N/m and 9.885 $\times 10^{-11}$ g, respectively. The resonance frequency of the microbridges with a known mass of Au patterned on top was measured for gold squares with edge lengths between 300 nm × 300 nm (corresponding to an added mass of 5.211 x 10^{-13} g) and 1.6 µm × 1.6 µm (corresponding to an added mass of 1.544 x 10^{-11} g) and is plotted in fig. 2(a). A continuous decrease in f_r was observed with increase in mass of Au from 10 pg to 154 pg. Below 10 pg, no significant change of f_r was observed, and the scatter is dominated by sample-to-sample variations. The dashed line in fig. 2(a) shows the expected variation in f_r as a function of the mass of the Au squares. Expected values of $f_r = f_i + \Delta f_r$ were arrived at by calculating the initial resonance frequency f_i using eq. (1) and considering m as the mass of the microbridge without any Au on top. Δf_r was calculated for the known Δm using eq. (2). As shown in fig. 2(a), there is only qualitative agreement between the experimental and the calculated values. This deviation is expected because factors like sample-to-sample variation in their rigidity ($(EI)_{eff}$) and geometry, the effect of the Au squares on the rigidity of the microstructure, the likely presence of residual stresses, the effective boundary conditions of the microstructure, and its 2D characteristic were not considered in these simple calculations.

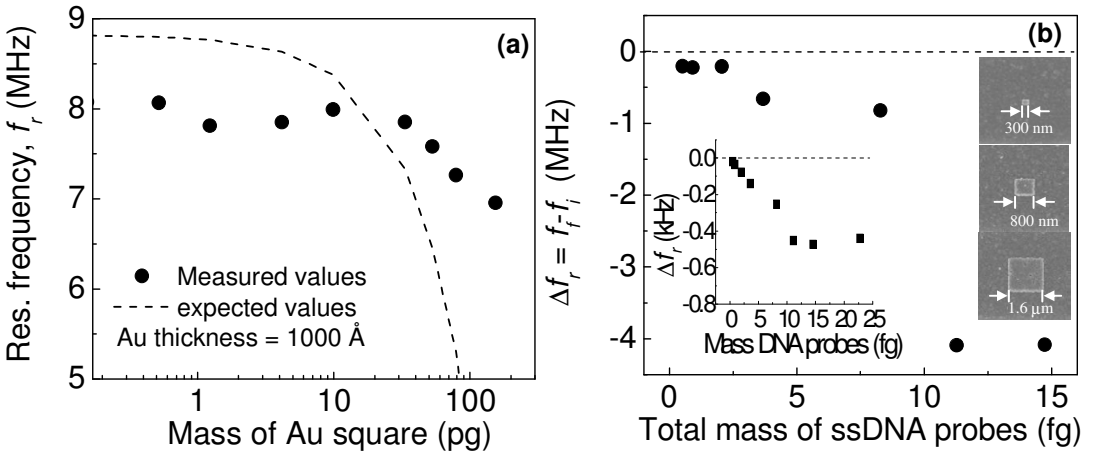

Fig. 2 (a) Variation of f_r as a function of the mass of the Au square. The dotted line shows calculated values for f_r. (b) Change in the resonance frequency, Δf_r of the micro-bridge after immobilization of the ssDNA probe on the Au squares on top of the microbridge as a function of the mass of ssDNA probes (which is proportional to the area of the Au square). The inset in figure shows the calculated values for the Δf_r considering a typical DNA immobilized density and exclusively mass loading effects. SEM micrographs of the Au squares are also shown in the inset.

2.1. Immobilization of ssDNA probes

The Au surface of the patterned square on top of the micro-bridge was used for the specific immobilization of thiolated ssDNA probes. 1 μM solution of ssDNA probes was prepared in Tris EDTA (TE) buffer (pH~ 7.4) and immobilization was performed at 37 °C for 2 hours. The resonance frequency of the micro-bridges was measured before and after immobilization of the ssDNA probes and the change in frequency is shown in fig. 2(b) as a function of the mass of the calculated total number of probes immobilized on the Au squares of different areas. The total mass of the ssDNA probes was calculated considering a standard immobilization density of 3×10^5 probes/μm^2 and the mass of one probe as 1.92×10^{-11} ng [8]. This calculated mass is proportional to the area of the Au squares where the immobilization took place. An estimated minimum mass of the immobilized ssDNA probes of ~ 2 fg was measured using these microresonators. The increased sensitivity in this experiment as compared to the previous experiment with Au squares results because these shifts are measured on the same sample and so sample to sample variations do not come into play as was the case in the results shown in fig. 2(a).

3. Conclusions

Bilayer TiW/a-Si:H microbridges were fabricated on glass substrates using Al sacrificial layer with Au squares patterned on top. The mass of the Au square on a microbridge down to 20 pg was measured and was limited by significant sample-to-sample variation in their resonance frequency. A mass of specifically immobilized thiolated ssDNA probes as low as 2 fg was measured.

Acknowledgements

The authors gratefully acknowledge S. Cardoso, F. Silva, V. Soares and J Bernardo for help in sample/cleanroom processing; J. Borme for help with SEM; and V. Martins for help with an immobilization of ssDNA. S. Patil thanks Fundação para a Ciência e Tecnologia (FCT) for a post-doctoral grant (grant no. SFRH/BPD/37466/2007). This work was supported by Fundação para a Ciência e a Tecnologia (FCT) through research projects and through the Associated Laboratory, IN.

References

1. P. S. Waggoner and H. G. Craighead, “micro- and nano mechanical sensors for environmental, chemical and bio-logical detection”, *Lab on a chip* 2007; **7**: 1238-1255.
2. Burg T P, Godin M, Knudsen S M, Shen W, Carlson G, Foster J S, Babcock K, Manalis S R, “Weighing of biomolecules, single cells and single nanoparticles in fluid,” nature letters 2007; **446**: 1066.
3. Yang Y T, Callegari C, Feng X L, Ekinci K L & Roukes M L, “Zeptogram-scale nanomechanical mass sensing”, Nano Lett. 2006; **6**: 583 - 586.
4. Naik A K, Hanay M S, Hiebert W K, Feng X L & Roukes M L, “Towards single-molecule nanomechanical mass spectrometry” Nature Nanotechnology, (Published online: 21 June 2009 | doi:10.1038/nnano.2009.152).
5. Gaspar J, Chu V and Conde J P, “High quality factor amorphous silicon electrostatic microresonators”, *Appl. Phys. Lett*. 2004; **84**: 622.
6. Guedes A, Patil S B, Cardoso S, Chu V, Conde J P and Freitas P P, “Hybrid magnetoresistive/ micro-electromechanical devices for static field modulation and sensor 1/f noise cancellation”, *Journal of Applied Physics* 2008;**103**: 07E924.
7. Gaspar J, Chu V and Conde J P, “Electrostatic actuation of thin-film microelectromechanical structures”, *J. Appl. Phys.* 2003; **93**: 10018.
8. Martins V. Ph. D. thesis, INESC-microsistemas e nanotecnologias, Lisbon, 2009.